Dynamics of gap solitons in one-dimensional binary lattices with saturable self-defocusing nonlinearity and alternating spacing

Petra P. Beličev,[1] Igor Ilić,[1] Aleksandra Maluckov,[1] Milutin Stepić,[1] Andrey Kanshu,[2] Christian E. Rüter,[2] and Detlef Kip[2]
[1]*P* Group, Vinča Institute of Nuclear Sciences, University of Belgrade, P.O. Box 522, 11001 Belgrade, Serbia*
[2]*Faculty of Electrical Engineering, Helmut Schmidt University, 22043 Hamburg, Germany*
(Received 2 August 2012; published 24 September 2012)

The existence and stability of spatial solitons in one-dimensional binary photonic lattices with alternating spacing and a saturable defocusing type of nonlinearity are investigated. Five types of nonlinear localized structures are found to exist: two in the mini-gap in the energy spectrum and others in the regular gap. It is proved that some of them are stable in certain ranges of the system parameters. Interactions between two identical localized structures propagating parallel to each other are investigated, too. It is shown that this interaction leads to formation of different localized patterns, such as solitons, breather-like modes, and breather complexes. The interaction output depends on the power and type of interacting identical solitons, the separation between them, the width of the mini-gap, and the phase relation between the tails of interacting solitons.

DOI: 10.1103/PhysRevA.86.033835 PACS number(s): 42.65.Tg, 42.65.Wi, 42.82.Et, 63.20.Pw

I. INTRODUCTION

One-dimensional (1D) photonic crystals or photonic lattices (PLs) represent a special type of optical waveguide array in which it is possible to control the propagation of light by changing the parameters of the system, such as the refractive index and lattice period. The periodic lattice system is characterized by discrete translation symmetry which determines the band-gap structure of the energy spectra, i.e., the creation of allowed and forbidden bands for the propagation of light [1]. This concept is similar to that developed in solid state physics for electrons moving through a crystalline lattice [2]. Due to their configuration, PLs exhibit various phenomena that cannot be observed in homogenous optical media, such as discrete diffraction and Bloch oscillations [3] or diffraction management [4]. In nonlinear PL media the interplay between nonlinear and linear effects can lead to a localization of energy into a few channels. Moreover, nonlinearity can influence the system to develop modulational instability [5,6] or cause creation of lattice solitons [7–9] and interactions among them [10–12].

Inexhaustible investigation of the possible ways to control the transport properties of light led to the development of different types of PLs, such as lattices with various defects [13–15], curved [16] and zig-zag [4] PLs, lattices with alternating positive and negative couplings between neighboring channels [17], or those exhibiting parity-time symmetry [18]. Recently, there has been a lot of interest in binary PLs—a special type of nonuniform PL whose additional periodicity gives rise to an extra mini-gap [19] in the corresponding spectra. One-dimensional binary PLs were examined both theoretically and experimentally in structures composed of optical waveguides with alternating widths [20–22] or periodically modified spacing between them [23–25]. In both configurations mini-gaps occur and an additional narrow frequency region for formation of (mini-) gap solitons opens. Furthermore, Bloch-Zener oscillations [26] as well as properties of surface localized modes [27,28] in various binary superlattices have been studied, too.

Soliton interactions and their propagation in different directions through PLs attract a lot of attention in the study of optical soliton phenomena [29]. There are two types of soliton interactions to be distinguished: coherent and incoherent ones. Coherent interactions occur in materials with an instantaneous (or extremely fast) nonlinear response, like the case of Kerr or quadratic nonlinearities. For coherent interactions it is important that the relative phase between the two beams that overlap and interfere stays fixed for durations much longer than the response time of the medium's nonlinearity [30]. In that case solitons may attract or repulse depending on whether their envelopes are in phase or out of phase. Furthermore, interesting behavior of anomalous coherent interactions of spatial gap solitons in optically induced photonic lattices has also been demonstrated [31,32]. On the other hand, in the case of incoherent interactions the relative phase change between the beams is much faster than the nonlinear response of the material. Incoherent interactions were studied intensively using materials with slow nonlinear response such as photorefractive crystals [33]. However, if the relative phase between the interacting solitons is held constant during their propagation, coherent interaction may occur even in photorefractive media [34,35]. Various phase-dependent interactions between solitons open up a vast research area of soliton dynamics such as switching, steering, and propagation control in photonic lattices [36–38].

In this paper, we extend our analysis of light propagation in a binary lattice with saturable nonlinearity and alternating spacing presented in Ref. [24], and we investigate how the variation in the lattice period, i.e., the coupling between channels, affects the band-gap structure, formation, and interaction of (mini-) gap solitons. Our results show the existence of five different types of nonlinear localized modes, two of which exist in the mini-gap, while all others appear in the regular gap. Furthermore, stability of (mini-) gap solitons is briefly discussed. In addition, we study numerically parallel interactions between identical gap solitons, looking for nonlinear all-optical switching in such double-periodic PLs. Depending on the type of interacting solitons, mutual phase relation, as well as the distance between them, attractive and repulsive interactions can be observed, leading to the fusion of two solitons into a single one or forcing them to change propagation course through the lattice.

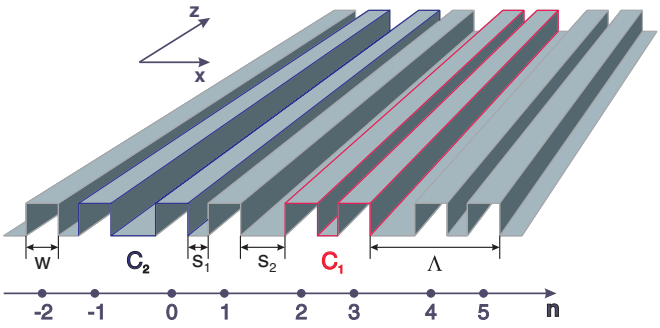

FIG. 1. (Color online) Schematic representation of a binary PL consisting of $2N$ elements with constant channel width w and alternating separations s_1 and s_2. The basic unit cell of the lattice (two channels coupled via C_1) is highlighted in red. The period of the binary PL is denoted by Λ.

II. THE MODEL

Our model describes the light propagation in a 1D binary PL composed of $2N$ identical channels whose mutual distance periodically changes, as depicted in Fig. 1. This setup can be viewed as an array comprising coupled two-channel basic cells, whereby each basic cell includes channels coupled via a coupling constant C_1. Coupling between cells is then described by another coupling constant, C_2.

If we presume light propagation along the z direction, the field evolution can be described by the discrete nonlinear Schrödinger equation (DNSE) with a saturable nonlinear term [39]:

$$i\frac{dE_n(z)}{dz} + C_{n,n-1}E_{n,n-1}(z) + C_{n,n+1}E_{n,n+1}(z) + \alpha\frac{|E_n(z)|^2}{1+\kappa|E_n(z)|^2}E_n(z) = 0, \quad (1)$$

where n denotes the index of the channel in the lattice, $E_n(z)$ is the mode amplitude in the nth channel, while $\alpha = -1$ and κ represent nonlinear coefficient describing a defocusing type of nonlinearity and saturation parameter, respectively. The two conserved quantities of the system are the total power $P = \sum_n |E_n|^2$ and the Hamiltonian $H = \sum_n[-C_{n,n-1}E_{n-1}E_n^* - C_{n,n+1}E_{n+1}E_n^* - \alpha|E_n|^2/\kappa + \alpha\ln(1+\kappa|E_n|^2)/\kappa^2]$.

Following the procedure presented in Ref. [18], in the linear regime ($\alpha = 0$) we separately observe the modes' evolution in even ($E_n = a_n$) and odd ($E_n = b_n$) elements of the lattice and reduce the 1D DNSE to two coupled sets of equations:

$$\begin{aligned} i\frac{da_n}{dz} + C_2 b_{n,n-1} + C_1 b_{n,n+1} &= 0, \\ i\frac{db_n}{dz} + C_1 a_{n,n-1} + C_2 a_{n,n+1} &= 0. \end{aligned} \quad (2)$$

Stationary light propagation requires field amplitudes in the form $a_n = A\exp[i(K_b n\Lambda - \beta z)]$ and $b_n = B\exp[i(K_b n\Lambda - \beta z)]$, where β, K_b, and Λ stand for the propagation constant of a mode, the Bloch momentum, and the period of the lattice, respectively. By replacing the presumed solutions into Eq. (2), the following dispersion relation can be derived:

$$K_b = \frac{1}{2\Lambda}\arccos\left(\frac{\beta^2 - (C_1^2 + C_2^2)}{2C_1C_2}\right). \quad (3)$$

The frequency regions of bands and gaps are determined by the value of K_b. Bands in the spectrum demand real K_b, while for the complex values of K_b corresponding gaps occur. From Eq. (3) it follows that the Bloch momentum has complex values for $\beta \in (-(C_1 - C_2),(C_1 - C_2))$ and $\beta \in ((C_1 + C_2),\infty)$. Unlike in a uniform PL, the spectrum of a binary PL is characterized by the existence of two gaps, whereby the position of the gaps is imposed by the corresponding intervals for β. This division of the first band and emergence of a mini-gap are the consequences of the additional modulation of the refractive index, which is modeled by alternating changes in the values of the coupling constants. The dependence of the width of a mini-gap on the coupling constants is governed by $d_{mg} = 2(C_1 - C_2)$. For the reference lattice, we set the coupling constants to be $C_1 = 282\ \mathrm{m}^{-1}$ and $C_2 = 127\ \mathrm{m}^{-1}$ as in Ref. [24]. By holding the first parameter fixed and varying the second one, it is evident that the energy spectrum of the binary lattice changes, making the mini-gap broader or narrower,

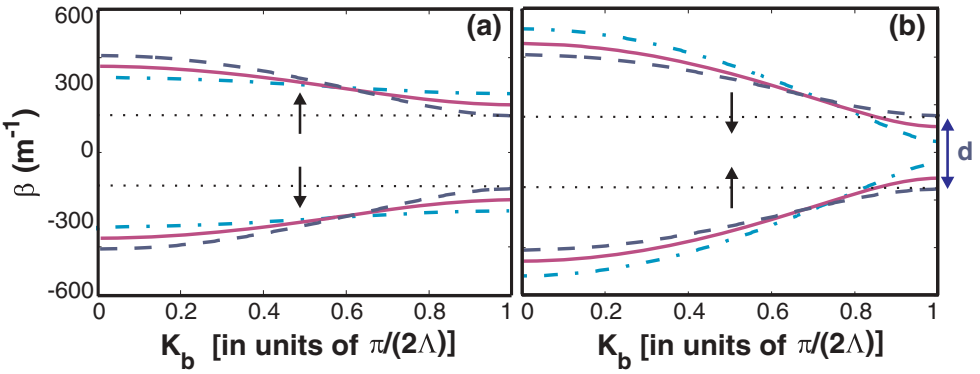

FIG. 2. (Color online) Comparative illustration of the band-gap spectra for binary PLs with (a) broader and (b) narrower mini-gap widths with respect to the reference lattice whose mini-gap width is denoted by d ($C_1 = 282\ \mathrm{m}^{-1}$, $C_2 = 127\ \mathrm{m}^{-1}$, dashed dark blue line). The left panel depicts results obtained for binary PLs with $C_2 = 80.5\ \mathrm{m}^{-1}$, $d_{mg} = 1.3d$ (purple solid line), and $C_2 = 34\ \mathrm{m}^{-1}$, $d_{mg} = 1.6d$ (dash-dotted light blue line). On the right panel calculated results are given for binary PLs with $C_2 = 173.5\ \mathrm{m}^{-1}$, $d_{mg} = 0.7d$ (purple solid line) and $C_2 = 235.5\ \mathrm{m}^{-1}$, $d_{mg} = 0.3d$ (dash-dotted light blue line). The coupling coefficient $C_1 = 282\ \mathrm{m}^{-1}$ has a fixed value in all cases. Arrows in the panels show directions of the mini-gap growth (left) and reduction (right).

depending on the mutual ratio between C_1 and C_2 (Fig. 2). It can be noticed that by decreasing the ratio between the coupling constants the mini-gap becomes more narrow, until finally it disappears, leading to the case of an uniform lattice.

III. NONLINEAR LOCALIZED MODES

The stationary solutions of Eq. (1) can be written in the form $E_n(z) = E_n \exp(-i\beta_{nl} z)$, with β_{nl} being the corresponding nonlinear propagation constant inside the gap. We solve this problem using a procedure based on the Gauss-Newton algorithm [40]. In the following, we distinguish five different types of nonlinear localized modes: two in the mini-gap and three in the region of the regular gap. For simplicity, we termed solitons from the mini-gap as MG solitons of types I and II. In the regular gap we distinguish antisymmetric solitons of types I and II and twisted modes. The distinction between types I and II refers to the position of the center of the localized structure: type I solitons identify structures whose centers are positioned within the lattice cell, while type II identifies solitons whose centers are located between two neighboring cells. Apart from obtaining numerical solutions, we made analytical estimations for narrow localized structures and derived corresponding expressions.

The stability of localized modes is considered with respect to three criteria: the spectral criterion obtained by a linear stability analysis (LSA) [41], the criterion derived from the Hamiltonian versus power (H-P) diagrams [42], and the numerical criterion. The last one is based on the results of a direct numerical simulation of the propagation of initially slightly perturbed localized modes. Here, the model equation (1) is numerically solved by a fifth-order Runge-Kutta procedure [43]. The total simulation length is set to $z = 400$ mm, which by far exceeds experimentally accessible lengths in nonlinear crystal samples. The spectral criterion, based on the linearization with respect to small perturbations, and H-P criterion cannot give a definite answer for the nonlinear system stability. Therefore, here the stability of modes is determined by direct numerical simulation.

A. Mini-gap solitons

Mini-gap solitons are found to exist for nonlinear propagation constants inside the extra gap. They are characterized by a field amplitude that is in phase within the unit cell, and they have a phase jump of π among neighboring cells. The numerically obtained field profiles of both types of MG solitons are depicted in Figs. 3(a) and 3(b).

Following the numerically obtained MG soliton patterns of type I, we derived simple analytical expressions for the field amplitudes, and we checked whether they fit the numerical counterparts. The starting amplitude configuration was $(E_{-(N-1)}, E_{-(N-2)}, \ldots, E_{-4}, E_{-3}, -E_{-2}, -E_{-1}, E_0, E_1, -E_2, -E_3, E_4, E_5, \ldots, E_{N-1}, E_N)$, and we assumed that the field amplitude E_n has the most significant values in the first and third channels [as in Fig. 3(a)]. Including this into the system of equations (1) and keeping only the largest terms, after a straightforward algebraic procedure we obtained the

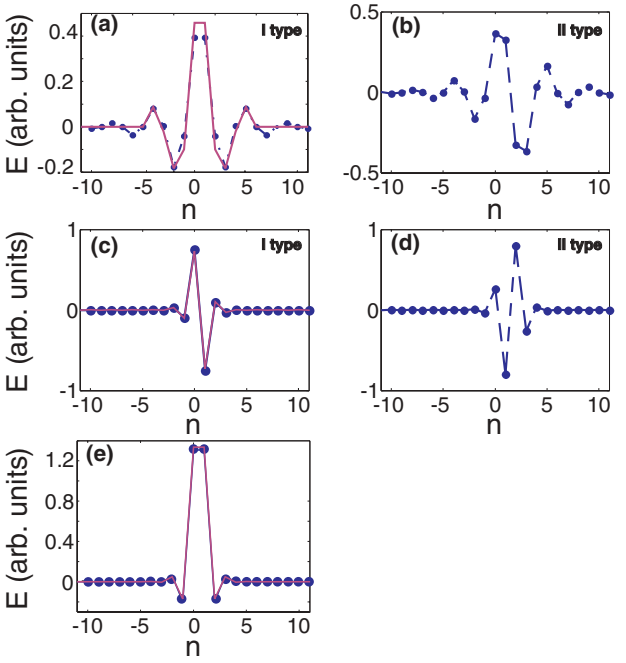

FIG. 3. (Color online) Field profiles of MG solitons of type I (a) and II (b), antisymmetric solitons of type I (c) and type II (d), and a twisted soliton (e) for a reference lattice $C_1 = 282$ m^{-1}, $C_2 = 127$ m^{-1}, and $\kappa = 5 \times 10^{-4}$. Field amplitudes are in arbitrary units and scaled by the factor $\sqrt{\kappa}$. Dashed lines with circles and solid lines denote the numerical and analytical results, respectively.

amplitudes of the MG solitons of type I:

$$E_1 = \sqrt{\frac{-(\beta_{nl} + C_1)}{\alpha + \kappa(\beta_{nl} + C_1)}}, \quad E_3 = \sqrt{\frac{-\beta_{nl}}{\alpha + \beta_{nl}\kappa}},$$

$$E_2 = \frac{C_2 E_1 - C_1 E_3}{\beta_{nl}}, \quad E_4 = \frac{\beta_{nl} C_2}{\beta_{nl}^2 - C_1^2} E_3,$$

$$E_{n=2j+3} = \left(\frac{C_1}{\beta_{nl}}\right)^j \left(\frac{C_2}{\beta_{nl}}\right)^{j-1} E_4 \quad (j = 1, \ldots, N/2 - 2),$$

$$E_{n=2j+4} = \left(\frac{C_1}{\beta_{nl}}\right)^j \left(\frac{C_2}{\beta_{nl}}\right)^{j} E_4 \quad (j = 1, \ldots, N/2 - 2).$$

Since the MG soliton of type I is symmetric with respect to the central cell, the same amplitude distribution will be valid for $n = -(N-1), \ldots, 0$. In contrast to numerically obtained solutions that are found in the whole mini-gap, approximate analytical solutions exist only for $\beta_{nl} \in (0, C_1 - C_2)$ [see Fig. 4(a)].

The analytical results nicely reproduce only the central part of the soliton structure (up to the fifth element) [see Fig. 3(a)], and the corresponding power can be written in the form

$$P_{MG} \approx 2\Bigg[|E_1|^2 + |E_2|^2 + |E_3|^2\left(1 + \frac{\beta_{nl}^2 C_2^2}{\left(\beta_{nl}^2 - C_1^2\right)^2} + \frac{C_1^2 C_2^2}{\left(\beta_{nl}^2 - C_1^2\right)^2}\right)\Bigg], \quad (4)$$

which exhibits larger deviations compared to the numerical curve.

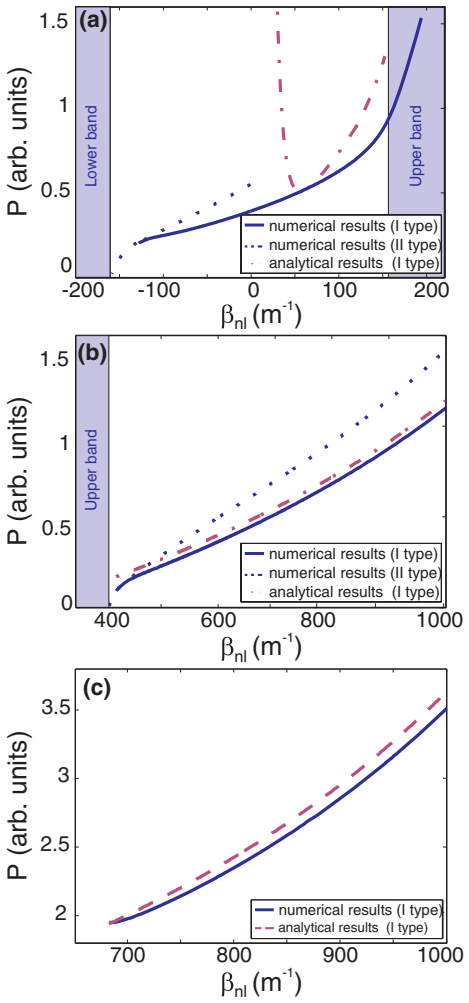

FIG. 4. (Color online) Power vs β_{nl} for (a) MG, (b) antisymmetric, and (c) twisted solitons for the reference lattice parameters $C_1 = 282\ \mathrm{m}^{-1}$, $C_2 = 127\ \mathrm{m}^{-1}$, and $\kappa = 5 \times 10^{-4}$. Power is given in arbitrary units and scaled by the factor κ.

The existence curves of the MG solitons, obtained numerically, are depicted in Fig. 4(a). It can be seen that there are two solution branches, each corresponding to a certain type of MG localized mode. The solid blue curve in Fig. 4(a) defines the existence region of the MG modes of type I. It extends throughout the entire mini-gap. The MG solitons close to the upper band slowly converge to "outgap" solitons [44], which are characterized by nondecaying tails. The analytically estimated curve for the MG solitons of type I is shown in this plot as a red dashed curve. On the other hand, type II MG solitons [dotted blue curve in Fig. 4(a)] exist only for negative values of β_{nl}. In addition, results show that the soliton power for type I solitons decreases with the increase of d_{mg}. However, the power of modes of type II increases for broader mini-gaps.

The linear stability analysis showed that the MG solitons of type I are stable for negative values of β_{nl} and oscillatory unstable in almost the whole existence region characterized by a positive β_{nl}. These results are confirmed by direct numerical simulations, while the H-P criterion predicts stability of the MG solitons in the whole existence region. The type II solutions are unstable in the whole region of their existence for PLs whose mini-gap widths are less than d according to the LSA and direct numerical simulations. For lattices with broader mini-gap, there is an area of frequencies for which the LSA predicts stable propagation of solitons. While this is consistent with the H-P criterion, numerical simulations show instability of these solutions after $z = 200$ mm.

B. Antisymmetric solitons

In the regular gap, we numerically obtained two types of antisymmetric soliton solutions. The type I solution is derived analytically, too. Both types of modes exhibit a pure staggered form [Figs. 3(c) and 3(d)]. The following analytical solutions for the amplitude of modes of type I have been obtained starting with the amplitude pattern $(E_{-(N-1)}, \ldots, E_{-2}, -E_{-1}, E_0, -E_1, E_2, \ldots, E_N)$ and assuming $|E_0| = |E_1| \gg |E_n|$, $n = -1, \pm 2, \pm 3, \ldots$:

$$E_1 = \sqrt{\frac{\beta_{nl} - C_1}{-\alpha + \kappa(C_1 - \beta_{nl})}},$$

$$E_{n=2j} = \frac{C_2^j C_1^{j-1}}{\beta_{nl}^{2j-1}} E_1 \quad (j = 1, \ldots, N/2),$$

$$E_{n=2j+1} = \frac{C_2^j C_1^j}{\beta_{nl}^{2j}} E_1 \quad (j = 1, \ldots, N/2 - 1),$$

with the corresponding power

$$P_{as} = 2|E_1|^2 \left[\sum_{j=1}^{N/2} \left(\frac{C_2}{\beta_{nl}} \right)^{2j-2} \left(\frac{C_1}{\beta_{nl}} \right)^{2j-2} + \sum_{j=1}^{N/2} \left(\frac{C_2}{\beta_{nl}} \right)^{2j} \left(\frac{C_1}{\beta_{nl}} \right)^{2j-2} \right]. \quad (5)$$

Due to the antisymmetry with respect to the central cell, mode amplitudes will be inversed for $n = -(N-1), \ldots, 0$. The existence region of this soliton type is $\beta_{nl} \in (C_1 + C_2, C_1 - \alpha/\kappa)$. Therefore, the analytically obtained profiles and the existence regions of type I antisymmetric solitons nicely fit the numerical findings, as illustrated in Figs. 3(c) and 4(b), where the latter one shows the corresponding $P(\beta_{nl})$ dependencies.

Similar to the case of MG solitons, two branches of the antisymmetric solutions can be distinguished. It is evident that the type II solitons require higher powers in order to be localized. For both types of solutions the increase of the mini-gap's width causes an increase of power needed for nonlinear localization.

The stability of the antisymmetric modes of type I is predicted by the H-P criterion in the whole existence region. However, according to the direct numerical simulations and the LSA, only the modes with low power are stable, while the high-power solutions are unstable and propagate as breathers. On the other hand, the LSA and direct numerical simulation indicate the instability of the solutions of type II in the whole region of their existence.

C. Twisted solitons

Besides antisymmetric modes, in the regular spectrum also gap twisted solitons exist. An example of a field profile of a twisted mode is depicted in Fig. 3(e). The envelope of a twisted solution is in phase within the central cell, while among neighboring elements of the lattice a phase shift of π appears [45], i.e., $(E_{-(N-1)},\ldots,E_{-2},-E_{-1},E_0,E_1,-E_2,E_3,\ldots,E_N)$. By adopting the analytical approach mentioned in the two previous sections for other soliton types, we obtained the following results for the corresponding amplitudes:

$$E_1 = \sqrt{\frac{-(\beta_{nl}+C_1)}{\alpha+\kappa(\beta_{nl}+C_1)}},$$

$$E_{n=2j} = \frac{C_2^j C_1^{j-1}}{\beta_{nl}^{2j-1}} E_1 \quad (j=1,\ldots,N/2),$$

$$E_{n=2j+1} = \frac{C_2^j C_1^j}{\beta_{nl}^{2j}} E_1 \quad (j=1,\ldots,N/2-1),$$

with the related power

$$P_{tw} = 2|E_1|^2 \left[\sum_{j=1}^{N/2} \left(\frac{C_2}{\beta_{nl}}\right)^{2j-2} \left(\frac{C_1}{\beta_{nl}}\right)^{2j-2} + \sum_{j=1}^{N/2} \left(\frac{C_2}{\beta_{nl}}\right)^{2j} \left(\frac{C_1}{\beta_{nl}}\right)^{2j-2} \right]. \quad (6)$$

These solutions exist for $\beta_{nl} \in (C_1+C_2,-C_1-\alpha/\kappa)$. Similar, due to the symmetric nature of the solution, mode amplitudes will be identical for $n=-(N-1),\ldots,0$ with respect to the central cell. The previous condition related to the analytically obtained β_{nl} interval implies the existence of twisted solitons in the regular gap. Obviously, this region of nonlinear propagation constants is in full accordance with the one obtained numerically. The curves of soliton existence [Fig. 4(c)] refer to a certain power threshold necessary for formation of twisted solitons. In this β_{nl} interval, analytical and numerical results are in good agreement. A decrease of the ratio C_1/C_2, i.e., a more narrow mini-gap, leads to a decrease of soliton power. Finally, for very narrow mini-gaps ($d_{mg}=0.3d$) no twisted modes are found to exist.

The stability of twisted modes is confirmed by all stability criteria in almost the whole existence region. Exceptions are the low-power modes whose instability is indicated by the LSA and numerical criteria.

IV. PARALLEL SOLITON INTERACTIONS IN BINARY PHOTONIC LATTICES

The understanding of soliton interactions in various PLs is of crucial significance for light manipulation in photonic devices. In this paper, we numerically investigate the parallel interactions of two identical localized modes of all existing types. In order to achieve interaction between two solitons, it is necessary that the mutual distance allows for an overlap of amplitude tails, so the localized modes can "feel" each other [37,46]. Depending on whether the tails of solitons are in phase or out of phase, the resulting interaction will have attractive or repulsive character. In general, the interaction output also depends on the solitons' power, the mini-gap width, and the initial distance Δ between the centers of two interacting solitons.

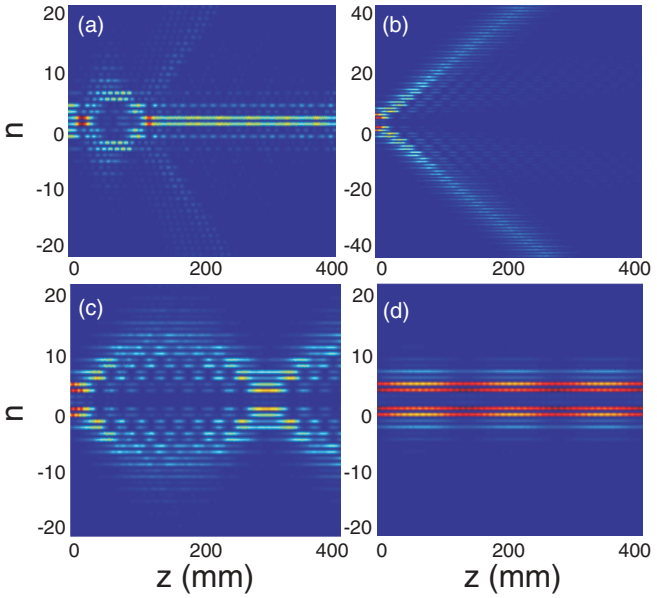

FIG. 5. (Color online) Top view of the parallel interactions between MG solitons of type I: (a) in-phase and (b) out-of-phase interaction in the reference lattice ($\beta_{nl}=-80\ \mathrm{m}^{-1}$), (c) out-of-phase interaction in a reference lattice ($\beta_{nl}=-20\ \mathrm{m}^{-1}$), and (d) out-of-phase interaction in the lattice with mini-gap width parameter $d_{mg}=1.3d$ ($\beta_{nl}=-100\ \mathrm{m}^{-1}$). In all cases the separation between centers of initial solitons equals $\Delta=2\Lambda$.

A. Interaction between MG solitons

In the case of the reference lattice, in-phase interactions between two MG solitons will lead to fusion of the interacting modes into narrow breather-like structures, mostly localized within one cell [Fig. 5(a)]. On the other hand, the out-of-phase solitons will repulse each other, causing the occurrence of discrete diffraction for low-power solitons, or free propagation across the lattice for solitons with higher powers, as shown in Fig. 5(b). These situations resemble those reported in Refs. [29,46]. Solutions which exist deeper in the mini-gap and whose tails are out of phase may form localized structures that will be deducted periodically and travel toward each other [Fig. 5(c)]. Simulations have shown that, with increasing the power of such solitons, the period of oscillations decreases. Observations of the interactions of MG solitons of type I with positive values of β_{nl} has pointed at their mutual attraction and formation of breather-like modes, no matter which type of interaction (in phase and out of phase) took part. A similar situation occurs for other types of examined binary PLs, whereby the in-phase interactions between solitons from broader mini-gaps and with $\beta_{nl}<0$ lead to fusion into a stable soliton of type I, while the out-of-phase interactions may cause formation of self-trapped breather complexes consisting of two coupled out-of-phase solitons with most of their energy concentrated within two cells [Fig. 5(d)].

In the case of interactions between MG solitons of type II, modes that are in phase attract each other, leading to the formation of localized structures with most of the energy

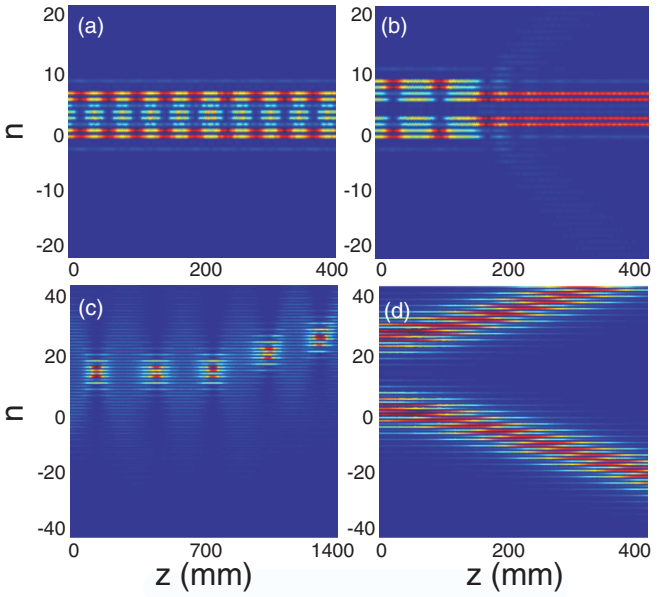

FIG. 6. (Color online) Top view of the parallel interactions between MG solitons of type II: (a) out-of-phase interaction ($d_{mg} = 1.3d$, $\Delta = 2\Lambda$, and $\beta_{nl} = -75\ \mathrm{m}^{-1}$), (b) out-of-phase interaction ($d_{mg} = 1.3d$, $\Delta = 3\Lambda$, and $\beta_{nl} = -75\ \mathrm{m}^{-1}$), (c) in-phase interaction ($d_{mg} = 0.3d$, $\Delta = 12\Lambda$, and $\beta_{nl} = -100\ \mathrm{m}^{-1}$), and (d) out-of-phase interaction ($d_{mg} = 0.3d$, $\Delta = 12\Lambda$, and $\beta_{nl} = -80\ \mathrm{m}^{-1}$).

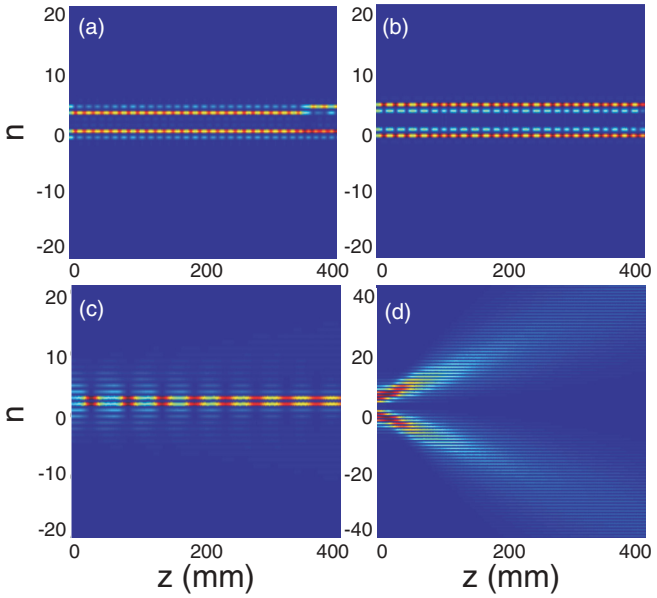

FIG. 7. (Color online) Top view of the parallel interactions in the reference lattice between antisymmetric solitons of type I: (a) in-phase interaction ($\beta_{nl} = 900\ \mathrm{m}^{-1}$), (b) out-of-phase interaction ($\beta_{nl} = 900\ \mathrm{m}^{-1}$), (c) in-phase interaction ($\beta_{nl} = 430\ \mathrm{m}^{-1}$), and (d) out-of-phase interaction ($\beta_{nl} = 430\ \mathrm{m}^{-1}$). In all cases the separation between centers of initial solitons equals $\Delta = 2\Lambda$.

localized within one cell, while the out-of-phase interactions have repulsive character. When the distance between centers of initial solitons equals two periods ($\Delta = 2\Lambda$), overlapping between structures is very strong, causing mutual transfer of energy. For these center separations, in-phase solitons give rise to fusion into a stable soliton mostly localized within one cell (low-power initial solitons) or narrow breather modes (high-power initial solitons). With the increase of the solitons' power, the out-of-phase interactions between solitons with center-to-center separation of $\Delta = 2\Lambda$ result in discrete diffraction for broad solitons, free propagation across the lattice for more localized initial modes, and interesting breather complexes for solitons that are deeper in the mini-gap, as depicted in Fig. 6(a). For larger separations $\Delta = 3\Lambda$, the overlap of tails decreases, as does the mutual influence. Now, the out-of-phase solitons that are deeper in the mini-gap construct stable soliton complexes with most of their energy located in two cells [Fig. 6(b)]. Reduction of the mini-gap affects the appearance of broad MG localized solutions of type II. To achieve the overlap of tails here, we took Δ to match 12 periods of the lattice in our calculations. Again, we varied the phase relation between the solitons' tails as well as the solitons' power. Simulations show that in-phase interactions between low-power solitons lead to periodical confinement of energy within several channels, as depicted in Fig. 6(c). On the other hand, the out-of-phase interactions cause repulsion of localized structures [Fig. 6(d)]. The narrower the initial solitons are, the less pronounced is the repulsion between them. With the increase of power more localized in-phase structures attract each other, an exchange of energy appears, and solitons continue to propagate freely through the lattice. With a further increase in the solitons' power, the solitons tend to fuse into a breather-like mode after they experience the first collision, whereby they collide later as the power of the solitons grows.

B. Interaction between antisymmetric solitons

In Figs. 7(a) and 7(b) the interactions (in phase and out of phase, respectively) between two very narrow antisymmetric solitons of type I are illustrated. Similarly to what was found in [46], the interaction causes a redistribution of energy between solitons, but it is not strong enough to force them to pass into other channels. Instead, two breather-like modes are formed whose oscillations in amplitude decrease with the increase of their mutual distance. As the power of the solitons decreases, which corresponds to broader localized structures, the interaction between them becomes more intense due to a greater overlap of tails. The perturbation to each of the solitons becomes larger, and in some cases it can lead to free movement of localized modes across the lattice. In these situations, the solitons are able to overcome the intralattice potential barrier [41,47]. For very broad modes, in-phase interactions will cause fusion into breather-like structures, while out-of-phase interacting solitons will lead to the occurrence of discrete diffraction, as illustrated in Figs. 7(c) and 7(d). With the increase of the mini-gap, interactions between antisymmetric modes of type I become weaker, whereupon most of the scenarios resemble the situations depicted in Figs. 7(a) and 7(b).

The type II soliton interactions are depicted in Fig. 8. Simulations show that besides the phase relation of interacting modes, the outcome of interactions considerably depends on the separation between centers of the initial structures and the width of the mini-gap, especially in cases of lattices with broader mini-gaps. For narrow mini-gaps, all in-phase

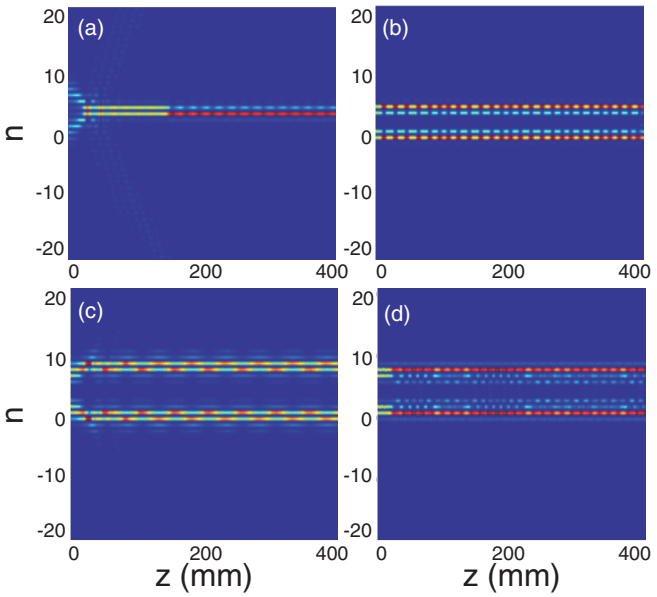

FIG. 8. (Color online) Top view of the parallel interactions between antisymmetric solitons of type II: (a) in-phase interaction and (b) out-of-phase interaction in a lattice with $d_{mg} = 0.3d$ ($\beta_{nl} = 600\ \mathrm{m}^{-1}$); (c) in-phase interaction and (d) out-of-phase interaction in a lattice with mini-gap width parameter $d_{mg} = 1.3d$ ($\beta_{nl} = 900\ \mathrm{m}^{-1}$). In all cases the separation between centers of initial solitons is $\Delta = 3\Lambda$.

interactions will cause fusion into breather-like modes with most of the energy concentrated within one cell, as illustrated in Fig. 8(a). Furthermore, very narrow localized structures will fuse into one-channel localized solitons. For out-of-phase interacting modes, mutual repulsion occurs, leading to a shift from initial channels and formation of breather-like complexes consisting of two self-trapped breather structures with most of the energy localized within basic cells (i.e., channels coupled via C_1), as presented in Fig. 8(b). With the increase of the solitons' power this repulsive character fades out, whereupon the amplitude oscillations of emerging breather structures decrease. On the other hand, in lattices with broad mini-gaps it is possible to obtain breather-like complexes with most of the energy trapped within two channels, which are symmetric with respect to the center of the breather complex [Fig. 8(d)]. This situation happens only if the interacting modes are narrow and sufficiently separated (at least $\Delta = 3\Lambda$). A similar situation is found for two narrow solitons whose tails are in phase and centers are positioned at $\Delta = 3\Lambda$. Here a breather complex is formed again, but now the peaks of the complex are closer to each other than in the case of out-of-phase interaction [Fig. 8(c)]. These phenomena may be suitable for applications in all-optical switching and light manipulation, following the concept of logic operations [48]. Also, in lattices with broad mini-gaps, low-power solitons with in-phase tails will form either a stable soliton of type I for $\Delta = 3\Lambda$ or a self-trapped breather for $\Delta = 2\Lambda$.

C. Interaction of twisted solitons

In the case of interactions between two identical twisted solitons, simulations show that the obtained localized structures do not feel each other for center separations Δ higher then three periods of the lattice. Furthermore, solitons found in the PLs with broad mini-gaps are highly localized, and thus for $\Delta > 2\Lambda$ interaction does not occur. In general, two identical high-power solitons with out-of-phase interacting tails will always change by transforming into two coupled breather-like modes. The in-phase interactions lead to the corruption of both structures and transport of energy through numerous channels in the lattice. The same situation happens for out-of-phase interactions between broad solitons. In addition, the interactions between high-power solitons are negligible in the PLs with broad mini-gaps.

V. CONCLUSION

In this work, we have analyzed localized mode formation and propagation of solitons through 1D binary PLs with alternating distances between adjacent elements and defocusing saturable nonlinearity. Due to the particular geometry of the binary lattice characterized by double periodicity, an additional mini-gap in the corresponding spectra is formed which enables the creation of new localized entities. Therefore, a new field of investigation and manipulation with newly localized patterns is opened. In addition, this sets huge challenges for experimental and theoretical investigations of the localized mode formation and propagation in complex multiperiodic lattices.

Here we demonstrate the existence of two types of mini-gap solitons, two types of antisymmetric gap solitons, as well as twisted gap solitons. The center of a mode of so-called type I is within the cell, while in the case of type II the center is located between two neighboring cells. The stability analysis, which is performed by a linear stability procedure, according to the H-P criterion and by direct numerical simulations, shows the existence of stable solitons under certain conditions. Here the exceptions are antisymmetric and MG solitons of type II, which are stable according to the LSA and H-P criterion but unstable according to the direct simulations. Finally, parallel interactions between two coherent identical solitons of the same type are studied. Direct simulations have shown the dependence of the interaction outcome on the solitons' power, mutual separation, phase relation between parts of the overlapping solitons' tails, as well as on the type of interacting solitons. Different situations may lead to the fusion of two solitons into another soliton or a narrow breather-like mode. Furthermore, scenarios such as mutual repulsion of solitons and formation of breather-like complexes are shown to be possible as well. This study is only an introduction to the intriguing field of localized structure management in multiperiodic photonic lattices.

ACKNOWLEDGMENTS

The authors acknowledge support from the Ministry of Education and Science of Republic of Serbia (Project III 45010) and the German-Serbian Academic Exchange Programme (DAAD Grants No. 54384481 and No. 680-00-00095/2012-09/5).

[1] J. D. Joannopoulos, S. G. Johnson, J. N. Winn, and R. D. Meade, *Photonic Crystals: Molding the Flow of Light*, 2nd ed. (Princeton University Press, Princeton, NJ, 2008).

[2] P. N. Prasad, *Nanophotonics* (Wiley, New York, 2004).

[3] R. Morandotti, U. Peschel, J. S. Aitchison, H. S. Eisenberg, and Y. Silberberg, Phys. Rev. Lett. **83**, 4756 (1999).

[4] H. S. Eisenberg, Y. Silberberg, R. Morandotti, and J. S. Aitchison, Phys. Rev. Lett. **85**, 1863 (2000).

[5] Yu. S. Kivshar and M. Peyrard, Phys. Rev. A **46**, 3198 (1992).

[6] J. Meier, G. I. Stegeman, D. N. Christodoulides, Y. Silberberg, R. Morandotti, H. Yang, G. Salamo, M. Sorel, and J. S. Aitchison, Phys. Rev. Lett. **92**, 163902 (2004).

[7] H. S. Eisenberg, Y. Silberberg, R. Morandotti, A. R. Boyd, and J. S. Aitchison, Phys. Rev. Lett. **81**, 3383 (1998).

[8] J. W. Fleischer, M. Segev, N. K. Efremidis, and D. N. Christodoulides, Nature (London) **422**, 147 (2003).

[9] J. W. Fleischer, G. Bartal, O. Cohen, T. Schwartz, O. Manela, B. Freedman, M. Segev, H. Buljan, and N. K. Efremidis, Opt. Express **13**, 1780 (2005).

[10] Z. Chen, M. Segev, T. H. Coskun, D. N. Christodoulides, and Yu. S. Kivshar, J. Opt. Soc. Am. B **14**, 3066 (1997).

[11] R. Morandotti, H. S. Eisenberg, D. Mandelik, Y. Silberberg, D. Modotto, M. Sorel, C. R. Stanley, and J. S. Aitchison, Opt. Lett. **28**, 834 (2003).

[12] E. Smirnov, M. Stepić, C. E. Rüter, V. Shandarov, and D. Kip, Opt. Lett. **32**, 512 (2007).

[13] B. Freedman, G. Bartal, M. Segev, R. Lifshitz, D. N. Christodoulides, and J. W. Fleischer, Nature (London) **440**, 1166 (2006).

[14] M. I. Molina and Yu. S. Kivshar, Opt. Lett. **33**, 917 (2008).

[15] P. P. Beličev, I. Ilić, M. Stepić, A. Maluckov, Y. Tan, and F. Chen, Opt. Lett. **35**, 3099 (2010).

[16] G. Lenz, I. Talanina, and C. M. de Sterke, Phys. Rev. Lett. **83**, 963 (1999).

[17] N. K. Efremidis, P. Zhang, Z. Chen, D. N. Christodoulides, C. E. Rüter, and D. Kip, Phys. Rev. A **81**, 053817 (2010).

[18] C. E. Rüter, K. G. Makris, R. El-Ganainy, D. N. Christodoulides, M. Segev, and D. Kip, Nat. Phys. **6**, 192 (2010).

[19] A. A. Sukhorukov and Yu. S. Kivshar, Opt. Lett. **27**, 2112 (2002).

[20] A. A. Sukhorukov and Yu. S. Kivshar, Phys. Rev. Lett. **91**, 113902 (2003).

[21] R. Morandotti, D. Mandelik, Y. Silberberg, J. S. Aitchison, M. Sorel, D. N. Christodoulides, A. A. Sukhorukov, and Yu. S. Kivshar, Opt. Lett. **29**, 2890 (2004).

[22] Y. Tan, F. Chen, P. P. Beličev, M. Stepić, A. Maluckov, C. E. Rüter, and D. Kip, Appl. Phys. B **95**, 531 (2009).

[23] R. A. Vicencio and M. Johansson, Phys. Rev. A **79**, 065801 (2009).

[24] A. Kanshu, C. E. Rüter, D. Kip, V. M. Shandarov, P. P. Beličev, I. Ilić, and M. Stepić, Opt. Lett. **37**, 1253 (2012).

[25] A. Kanshu, C. E. Rüter, D. Kip, J. Cuevas, and P. G. Kevrekidis, Eur. Phys. J. D **66**, 182 (2012).

[26] F. Dreisow, A. Szameit, M. Heinrich, T. Pertsch, S. Nolte, A. Tünnermann, and S. Longhi, Phys. Rev. Lett. **102**, 076802 (2009).

[27] D. Mihalache, D. Mazilu, Yu. S. Kivshar, and F. Lederer, Opt. Express **15**, 10718 (2007).

[28] Y. J. He, W. H. Chen, H. Z. Wang, and B. A. Malomed, Opt. Lett. **32**, 1390 (2007).

[29] G. I. Stegeman and M. Segev, Science **286**, 1518 (1999).

[30] J. P. Gordon, Opt. Lett. **8**, 596 (1983).

[31] S. Liu, P. Zhang, F.-J. Xiao, X.-T. Gan, and J.-J. Zhao, Chin. Phys. B **19**, 065203 (2010).

[32] S. Liu, Y. Hu, P. Zhang, X. Gan, F. Xiao, C. Lou, D. Song, J. Zhao, J. Xu, and Z. Chen, Opt. Lett. **36**, 1167 (2011).

[33] D. Anderson and M. Lisak, Phys. Rev. A **32**, 2270 (1995).

[34] W. Królikowski and S. A. Holmstrom, Opt. Lett. **22**, 369 (1997).

[35] H. Meng, G. Salamo, M. F. Shih, and M. Segev, Opt. Lett. **22**, 448 (1997).

[36] J. S. Aitchison, A. M. Weiner, Y. Silberberg, D. E. Leaird, M. K. Oliver, J. L. Jackel, and P. W. E. Smith, Opt. Lett. **16**, 15 (1991).

[37] W. Królikowski, B. Luther-Davies, and C. Denz, IEEE J. Quantum Electron. **39**, 3 (2003).

[38] W. J. Firth and A. J. Scroggie, Phys. Rev. Lett. **76**, 1623 (1996).

[39] E. Smirnov, C. E. Rüter, M. Stepić, V. Shandarov, and D. Kip, Opt. Express **14**, 11248 (2006).

[40] A. Björck, *Numerical Methods for Least Square Problems* (Society for Industrial and Applied Mathematics, Philadelphia, 1996).

[41] Lj. Hadžievski, A. Maluckov, M. Stepić, and D. Kip, Phys. Rev. Lett. **93**, 033901 (2004).

[42] N. Akhmediev, A. Ankiewicz, and R. Grimshaw, Phys. Rev. E **59**, 6088 (1999).

[43] W. H. Press, S. A. Teukolsky, W. T. Vetterling, and B. P. Flannery, *Numerical Recipes—The Art of Scientific Computing*, 3rd ed. (Cambridge University Press, New York, 2007).

[44] A. V. Gorbach and M. Johansson, Eur. Phys. J. D **29**, 77 (2004).

[45] S. Darmanyan, A. Kobyakov, E. Schmidt, and F. Lederer, Phys. Rev. E **57**, 3520 (1998).

[46] A. B. Aceves, C. De Angelis, T. Peschel, R. Muschall, F. Lederer, S. Trillo, and S. Wabnitz, Phys. Rev. E **53**, 1172 (1996).

[47] Yu. S. Kivshar and D. K. Campbell, Phys. Rev. E **48**, 3077 (1993).

[48] D. N. Christodoulides, F. Lederer, and Y. Silberberg, Nature (London) **424**, 817 (2003).